Oxyanion-Mediated Inhibition of Serine Proteases[†,||]

Steven R. Presnell,[‡] Girish S. Patil,[§] Cameron Mura,[||] Kevin M. Jude, Jennifer M. Conley, Jay A. Bertrand, Chih-Min Kam, James C. Powers, and Loren Dean Williams*

School of Chemistry & Biochemistry, Georgia Institute of Technology, Atlanta, Georgia 30332-0400

Received July 9, 1998; Revised Manuscript Received September 24, 1998

ABSTRACT: Novel aryl derivatives of benzamidine were synthesized and tested for their inhibitory potency against bovine trypsin, rat skin tryptase, human recombinant granzyme A, human thrombin, and human plasma kallikrein. All compounds show competitive inhibition against these proteases with K_i values in the micromolar range. X-ray structures were determined to 1.8 Å resolution for trypsin complexed with two of the para-substituted benzamidine derivatives, 1-(4-amidinophenyl)-3-(4-chlorophenyl)urea (ACPU) and 1-(4-amidinophenyl)-3-(4-phenoxyphenyl)urea (APPU). Although the inhibitors do not engage in direct and specific interactions outside the S1 pocket, they do form intimate *indirect* contacts with the active site of trypsin. The inhibitors are linked to the enzyme by a sulfate ion that forms an intricate network of three-centered hydrogen bonds. Comparison of these structures with other serine protease structures with noncovalently bound oxyanions reveals a pair of highly conserved oxyanion-binding sites in the active site. The positions of noncovalently bound oxyanions, such as the oxygen atoms of sulfate, are distinct from the positions of covalent oxyanions of tetrahedral intermediates. Noncovalent oxyanion positions are outside the "oxyanion hole." Kinetics data suggest that protonation stabilizes the ternary inhibitor/oxyanion/protease complex. In sum, both cations and anions can mediate K_i. Cation mediation of potency of competitive inhibitors of serine proteases was previously reported by Stroud and co-workers [Katz, B. A., Clark, J. M., Finer-Moore, J. S., Jenkins, T. E., Johnson, C. R., Ross, M. J., Luong, C., Moore, W. R., and Stroud, R. M. (1998) *Nature 391*, 608−612].

Trypsin-like serine proteases play critical roles in physiological processes such as blood coagulation, complement activation, digestion, fibrinolysis, kinin formation, reproduction, and phagocytosis (*2*). Inhibitors of trypsin-like enzymes are potentially useful in treating a variety of disease states, including coronary and cerebral infraction, vascular clotting, pancreatitis, arthritis, and tumor cell invasion (*3*, *4*). Potency and specificity can be attained by incorporating the small inhibitor benzamidine [$K_i = 35$ μM for bovine trypsin, 235 μM for human thrombin (*5*)] into larger and more complex inhibitors. Indeed, compounds such as NAPAP (*6*), 2,7-di-(4-amidinophenyl)methenyl cycloheptanone (*7*), and α,α'-bis(4-amidino-2-iodophenoxy)-*p*-xylene (*8*), which incorporate the amidinophenyl moiety, demonstrate submicromolar inhibition and high specificity for certain trypsin-like enzymes. Molecular interactions between these inhibitors and target enzymes have been defined in detail from three-dimensional structures of protease−inhibitor complexes (*9*, *10*). The amidinophenyl moiety of the inhibitor is invariably anchored by hydrogen bonds to an aspartic acid residue at the base of the primary specificity pocket (the S_1 pocket) and to other residues that form the walls of the pocket.

The interactions of inhibitors with serine proteases can be mediated by divalent cations (*11*). Stroud and co-workers recently noted that, upon addition of zinc(II), the K_is of certain amidinophenyl-based compounds are reduced by 4 orders of magnitude. X-ray structures reveal ternary inhibitor/cation/trypsin complexes with a zinc ion coordinated simultaneously by inhibitor and active-site residues of the protease. Here, we describe oxyanion mediation of inhibition of trypsin-like proteases. We present high-resolution X-ray structures of bovine β-trypsin inhibited with a novel class of aryl inhibitors incorporating an amidinophenyl moiety (Figure 1). In each structure, a well-ordered sulfate ion links inhibitor to protein via a complex network of hydrogen bonds. A pair of highly conserved binding sites for noncovalent oxyanions is revealed by comparison of our structures with previous serine protease structures containing noncovalently bound oxyanions within the active site. These oxyanion positions are distinct from the positions of oxyanions of covalently bound tetrahedral intermediate analogues. Inhibitory constants of all synthesized compounds for bovine trypsin, human thrombin, rat skin tryptase, human granzyme A, and human plasma kallikrein were found to be in the micromolar range. K_i values for bovine trypsin inhibition by several compounds were lowered from 3 to 7-fold by sulfate ions, consistent with conserved sulfate ion position and interactions in the 3-dimensional structures. Our results suggest that targeting oxyanions or other electronegative

[†] This work was supported in part by the U.S. Army Medical Research and Development Command under Contract DMAD17-89-C-9008 (J.C.P.) and a grant provided by the Georgia Tech/Emory Seed Grant Program (L.D.W.).

[||] The atomic coordinates have been deposited in the Brookhaven Protein Data Bank (entries 1BJU and 1BJV).

* Address correspondence to this author.

[‡] Current address: Department of Biology, The University of North Carolina at Chapel Hill, Chapel Hill, NC 27599.

[§] Current address: Lexmark International, 740 New Circle Road, Lexington, KY 40511. [||]Current address: Department of Chemistry and Biochemistry, University of California at Los Angeles, Los Angeles, CA 90095.

10.1021/bi981636u CCC: $15.00
Published on Web 11/12/1998

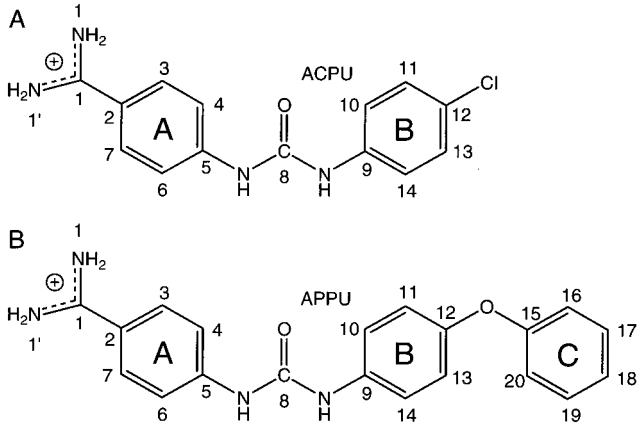

FIGURE 1: Covalent structure of (A) 1-(4-amidinophenyl)-3-(4-chlorophenyl)urea hydrochloride (ACPU) and (B) 1-(4-amidinophenyl)-3-(4-phenoxyphenyl)urea hydrochloride (APPU).

atoms to favorable positions in the active site of serine proteases may be a reasonable strategy for inhibiting trypsin-like proteases.

EXPERIMENTAL SECTION

Materials. Rat skin tryptase was provided by Dr. William H. Simmons, Loyola University Medical Center (Maywood, IL), human recombinant granzyme A by Dr. G. Duke Virca, Immunex Corporation (Seattle, WA), human α-thrombin by Dr. Sriram Krishnaswamy, Emory University (Atlanta, GA), and human plasma kallikrein by Dr. Kazuo Fuzikawa, University of Washington (Seattle, WA). Z-Lys-SBzl[1] and bovine trypsin was purchased from Sigma Chemical Company (St. Louis, MO). DTNB was purchased from Aldrich Chemical Co. (Milwaukee, WI). Z-Arg-SBzl was prepared as previously described (*12*). All other materials were purchased from Sigma (St. Louis, MO).

Synthesis. Unless otherwise noted, synthetic materials were obtained from commercial suppliers and used without further purification. The purity of each compound synthesized was determined by ^{1}H NMR spectroscopy, mass spectrometry, thin-layer chromatography, and melting point analysis. NMR chemical shifts (δ) are expressed in parts per million (ppm) with tetramethylsilane as the internal reference. Mass spectra were recorded on a Varian MAT 112S spectrometer. Elemental analyses were performed by Atlantic Microlabs (Atlanta). Thin-layer chromatography analyses were conducted on Baker IB2-F silica gel plates. Melting points were determined with a Büchi capillary apparatus. ^{1}H NMR spectra were recorded on a Varian Gemini 300. Methanol and 2-propanol were dried by distillation from CaH_2. THF and dimethoxyethane were dried by distilling from sodium benzophenone ketyl. Benzene was dried by distillation from lithium aluminum hydride. HCl was dried by passing through concentrated H_2SO_4 and $CaCl_2$. Ammonia was dried by passage through KOH.

Benzamidine derivatives were prepared by a modified Pinner reaction (*13*). The inhibitors are termed ureas or ethers, depending on the functional group linking the benzamidine and aromatic moieties. Synthesis of representative ureas and ethers are described below. The other benzamidine derivatives were prepared by appropriate substitution of the starting materials.

1-(4-amidinophenyl)-3-phenylurea (**1**). Phenylisocyanate (9.52 g, 0.08 mol) was added to a stirred solution of 4-aminobenzonitrile (4.72 g, 0.04 mol) in dry benzene (200 mL). The resulting solution was refluxed for 5 h and stirred further at room temperature overnight. The precipitated solid was filtered and recrystallized from methanol to yield the target urea derivative as a white crystalline solid (8.3 g).

Dry HCl vapor was passed through the urea described above (4.74 g, 0.02 mol) in dry dimethoxyethane (100 mL) and dry methanol (3.2 g, 0.01 mol) for 1 h. The reaction was stirred at room temperature for 24 h. The precipitated imidate ester (3.5 g) was filtered and stored over KOH in a vacuum desiccator for 24 h. The imidate ester (2 g, 0.006 mol) was dissolved in 2-propanol saturated with ammonia (100 mL) and the reaction mixture was refluxed for 6 h and stirred further at room-temperature overnight. The solvent was evaporated under reduced pressure, and the white solid obtained was recrystallized from 2 N HCl to yield the title compound as a HCl salt (1.5 g); mp 240 °C (decomp). ^{1}H NMR (DMSO-d_6): δ 7.00 (t, 1H), 7.30 (t, 2H), 7.45 (d, 2H), 7.65 (d, 2H), 7.80 (d, 2H), 8.80 (s, 2H), 9.15 (s, 2H), 9.40 (bs, 1H), 9.80 (bs, 1H). Anal calcd for $C_{14}H_{15}ClN_4O\cdot H_2O$: C, 54.53; H, 5.56; Cl, 11.35; N, 18.18. Found: C, 54.53; H, 5.46; Cl, 11.42; N, 18.13.

1-(4-Amidinophenyl)-3-(4-chlorophenyl)urea Hydrochloride (**2**). Mp 275 °C (decomp). ^{1}H NMR (DMSO-d_6): δ 7.32 (d, 2H), 7.50 (d, 2H), 7.66 (d, 2H), 7.80 (d, 2H), 8.85 (s, 2H), 9.18 (s, 2H), 9.70 (s, 1H), 9.98 (s, 1H). Anal calcd for $C_{14}H_{14}Cl_2N_4O\cdot 0.69\ H_2O$: C, 49.80; H, 4.58; Cl, 21.01; N, 16.59. Found: C, 50.21; H, 4.62; Cl, 20.73; N, 16.19.

1-(4-Amidinophenyl)-3-benzylurea Hydrochloride (**3**). Mp 292 °C (decomp). ^{1}H NMR (DMSO-d_6): δ 4.31 (d, 2H), 7.17 (t, 1H), 7.20−7.38 (m, 5H), 8.82 (s, 2H), 9.12 (s, 2H), 9.66 (s, 1H). Anal calcd for $C_{15}H_{17}ClN_4O$: C, 59.11; H, 5.62; Cl, 11.63; N, 18.38. Found: C, 59.23; H, 5.64; Cl, 11.63; N, 18.28.

1-(4-Amidinophenyl)-3-(4-phenoxyphenyl)urea Hydrochloride (**4**). Mp 202−205 °C. ^{1}H NMR (DMSO-d_6): δ 6.90−7.01 (m, 4H), 7.09 (t, 1H), 7.35 (m, 2H), 7.47 (m, 2H), 7.65(d, 2H), 7.80 (d, 2H), 8.80 (s, 2H), 9.15 (s, 2H), 9.39 (s, 1H), 9.75 (s, 1H). Anal calcd for $C_{20}H_{19}ClN_4O_2\cdot 0.75\ H_2O$: C, 60.60; H, 5.17; Cl, 8.96; N, 14.14. Found: C, 60.62; H, 5.19; Cl, 8.96; N, 14.05.

1-(3-Amidinophenyl)-3-phenylurea Hydrochloride (**5**). Mp 252−254 °C. ^{1}H NMR (DMSO-d_6): δ 6.98 (t, 1H), 7.20−7.35 (m, 3H), 7.40−7.55 (m, 3H), 7.70 (d, 1H), 7.95 (s, 1H), 9.1 (bs, 2H), 9.32 (bs, 2H), 9.45 (bs, 1H), 9.18 (bs, 1H). Anal calcd for $C_{14}H_{15}ClN_4O$: C, 57.83; H, 5.20 Cl, 12.19; N, 19.27. Found: C, 57.74; H, 5.20; Cl, 12.16; N, 19.21.

[1] Abbreviations: ACPU, 1-(4-amidinophenyl)-3-(4-chlorophenyl)-urea hydrochloride; APPU, 1-(4-amidinophenyl)-3-(4-phenoxyphenyl)-urea hydrochloride; DMSO, dimethyl sulfoxide; DTNB, 5,5′-dithiobis-(2-nitrobenzoic acid); HEPES, 4-(2-hydroxyethyl)-1-piperazineethanesulfonic acid; LT, low temperature; MES, 2-(*N*-morpholino)ethanesulfonic acid; NAPAP, N^{α}-(2-naphthylsulphonylglycyl)-*p*-amidinophenylalanylpiperidine; PPACK, D-Phe-Pro-Arg chloromethyl ketone; RT, room temperature; Z-Arg-SBzl, *N*−(benzyloxycarbonyl)arginylthiobenzyl ester; Z-Lys-SBzl, *N*−(benzyloxycarbonyl)lysinyl thiobenzyl ester; THF, tetrahydrofuran.

[2] The nomenclature of Schechter and Berger (*1*) is used to designate the residues (P_2, P_1, $P_{1'}$, $P_{2'}$, etc.) of a peptide substrate and the corresponding subsites (S_2, S_1, $S_{1'}$, $S_{2'}$, etc.) of the enzyme. The scissile bond is $P_1-P_{1'}$.

1-(3-Amidinophenyl)-3-(4-phenoxyphenyl)urea Hydrochloride (**6**). Mp 180−181 °C. ^{1}H NMR (DMSO-d_6): δ 6.91−7.20 (m, 4H), 7.10 (t, 1H), 7.30−7.40 (m, 3H), 7.45−7.58 (m, 3H), 7.70(d, 1H), 7.95 (s, 1H), 9.00 (s, 2H), 9.34 (s, 1H), 9.36 (s, 2H), 9.55 (s, 1H). Anal. calcd for $C_{20}H_{19}ClN_4O_2 \cdot 0.75\ H_2O$: C, 60.60; H, 5.17; Cl, 8.96; N, 14.14. Found: C, 60.62; H, 5.19; Cl, 8.96; N, 14.05.

(*4-Amidinobenzyl*)*benzyl Ether Hydrochloride* (**7**). A solution of benzyl alcohol (1.08 g, 0.01 mol) in dry THF (10 mL) was slowly added to sodium hydride (2.4 g, 0.10 mol). The suspension was stirred at room temperature for 15 min. A solution of α-bromo-*p*-tolunitrile (1.96 g, 0.01 mol) in 10 mL of dry THF was added dropwise, and this reaction mixture was stirred at room temperature for 24 h. Excess sodium hydride was carefully depleted by addition of water. The reaction mixture was suspended in ethyl acetate and the organic layer was washed with dilute HCl, then water, then brine, and dried over anhydrous magnesium sulfate. The organic layer was evaporated to obtain the liquid cyano ether.

Dry HCl was passed through a cooled solution of the cyano ether (1.00 g, 0.004 mol) and dry methanol (0.67 g, 0.020 mol) in dry dimethoxyethane (30 mL) for 1 h, and the reaction stored in a refrigerator for 16 h. The solvent was evaporated under reduced pressure. The imidate ester (1.0 g) obtained as a yellow solid was stored in a vacuum desiccator over KOH for 24 h. The imidate ester was dissolved in dry 2-propanol saturated with ammonia (50 mL), refluxed for 6 h, then stirred overnight. The solvent was evaporated from the solution, and the resulting solid was recrystallized from 2 N HCl to yield white crystals of the title compound (0.41 g, 44%), mp 102−104 °C. ^{1}H NMR (DMSO-d_6): δ 4.58 (s, 2H), 4.65 (s, 2H), 7.25−7.40 (m, 5H), 7.59 (d, 2H), 7.84 (d, 2H), 9.23 (bs, 2H), 9.41 (bs, 2H). Anal. calcd for $C_{15}H_{17}Cl_1N_2O$: C, 65.10; H, 6.19 Cl, 12.81; N, 10.12. Found: C, 64.98; H, 6.20; Cl, 12.73; N, 10.02.

(*4-Amidinobenzyl*)*phenylethyl Ether Hydrochloride* (**8**). Mp 147−150 °C. ^{1}H NMR (DMSO-d_6): δ 2.88 (t, 2H), 3.69 (t, 2H), 4.60 (s, 2H), 7.15−7.30 (m, 5H), 7.49 (d, 2H), 7.80 (d, 2H), 9.17 (bs, 2H), 9.37 (bs, 2H). Anal calcd for $C_{16}H_{19}ClN_2O$: C, 66.09; H, 6.59; Cl, 12.19; N, 9.63. Found: C, 66.18; H, 6.61; Cl, 12.09; N, 9.56.

(*4-Amidinobenzyl*)*phenylpropyl Ether Hydrochloride* (**9**). Mp 76−78 °C. ^{1}H NMR (DMSO-d_6): δ 1.84 (m, 2H), 2.62 (t, 2H), 3.45 (t, 2H), 4.55 (s, 2H), 7.10−7.90 (aromatic, 9H), 9.20 (bs, 2H), 9.45 (bs, 2H). Anal calcd for $C_{17}H_{21}ClN_2O$: C, 66.99; H, 6.94 Cl, 11.63; N, 9.19. Found: C, 67.05; H, 6.95; Cl, 11.54; N, 9.20.

(*4-Amidinobenzyl*)*3-phenoxylbenzyl Ether Hydrochloride* (**10**). Mp 109−112 °C; ^{1}H NMR (DMSO-d_6): δ 4.55 (s, 2H), 4.63 (s, 2H), 6.95−7.80 (aromatic, 13H), 9.16 (bs, 2H), 9.40 (bs, 2H). Anal calcd for $C_{21}H_{21}ClN_2O_2$: C, 68.38; H, 5.74; Cl, 9.61; N, 7.59. Found: C, 68.20; H, 5.78; Cl, 9.48; N, 7.44.

Bis(4-amidinophenyl)urea Dihydrochloride (**11**). A suspension of urea (0.60 g, 0.01 mol) and 4-aminobenzamidine (4.16 g, 0.02 mol) in water (5 mL) was heated under reflux for 24 h. The condenser was removed and the solution heated for an additional 24 h, after which the reaction was triturated with water (25 mL). The resulting solid was filtered and dissolved by heating in 150 mL of water to give a clear solution that was acidified with 30 mL of concentrated HCl and cooled to yield the product as a white solid (3.1 g, 84%); mp >250 °C. ^{1}H NMR (DMSO-d_6): δ 7.68 (d, 4H), 7.84 (d, 4H), 9.00 (s, 4H), 9.23 (d, 4H), 10.45 (s, 2H). Anal calcd for $C_{15}H_{18}Cl_2N_6O \cdot 0.3\ H_2O$: C, 48.07; H, 4.96; Cl, 18.96; N, 22.43. Found: C, 48.06; H, 5.05; Cl, 19.03; N, 22.55.

Enzyme Inhibition Kinetics, pH 7.5. Z-Arg-SBzl was used as the substrate for all enzyme assays except for rat skin tryptase, where Z-Lys-SBzl was used. In all assays, formation of the 4-nitro-3-carboxyphenylthiol chromophore was followed by monitoring absorbance increase at 410 nm (ϵ_{410} 14 173 $M^{-1}cm^{-1}$) with a Beckman 35 spectrophotometer. With the exception of tryptase, assays were carried out at 23 °C in a plastic cuvette containing 2.0 mL of buffer with 25 μL of inhibitor solution, 25 μL of substrate solution (either 5.0, 2.5, or 1.25 mM), and 150 μL of DTNB solution (20 mM) added. Inhibitor, substrate, and DTNB stocks were dissolved in DMSO. Tryptase assays were identical to that just described with the exception that 150 μL of DTNB solution (120 mM) was added to the cuvette. Reactions were initiated by addition of 25 μL of enzyme solution (~2.5 μM) to the cuvette. Buffers used in enzyme assays were the following: for trypsin, 0.1 M HEPES, pH 7.5, and 10 mM $CaCl_2$; thrombin, 0.1 M HEPES, pH 7.5, 0.5 M NaCl, and 0.1% PEG 6000; tryptase, 0.1 M HEPES, pH 7.5, 10% glycerol, and 10 μM heparin; granzyme A, 0.1 M HEPES, pH 7.5, and 10 mM $CaCl_2$; kallikrein, 0.1 M HEPES, pH 7.5, and 0.5 M NaCl. Each compound was assayed with trypsin, thrombin, or tryptase using duplicates of five inhibitor concentrations at three different substrate concentrations (30 samples/assay). Due to limited enzyme availability, duplicates of five inhibitor concentrations for two different substrate concentrations (20 samples) were utilized for granzyme A and kallikrein. K_i values for all assays were obtained from Dixon plots (*14*). K_i values for some of the derivatives tested against trypsin and tryptase have been published elsewhere (*15*), determined from two substrate concentrations.

Enzyme Inhibition Kinetics in the Absence or Presence of Sulfate. For assays carried out at pH 7.5, trypsin was assayed as described above except that the buffer utilized was 0.1 M HEPES, 5 mM $CaCl_2$, and either 0.2 M NaCl or 0.1 M Na_2SO_4, pH 7.5. For assays at pH 6.0, the buffer was 0.1 M MES, 5 mM $CaCl_2$, and either 0.2 M NaCl or 0.1 M Na_2SO_4, pH 6.0. Thrombin was assayed as described above except that buffer utilized was 0.1 M MES, 0.1% PEG 6000, and either 0.5 M NaCl or 0.3 M NaCl and 0.1 M Na_2SO_4, pH 6.0.

Crystallization. Bovine pancreatic β-trypsin was purified by the method of Schroeder and Shaw (*16*) as modified by Bode and Schwager (*10*). Fractions of β-trypsin were pooled, dialyzed against 5.0 mM MES, 1.0 mM $CaCl_2$, and 5.0 mM benzamidine, pH 6.0, and concentrated by ultrafiltration. Orthorhombic crystals were grown from 20 μL hanging drops containing 10−15 mg/mL β-trypsin, 1.0 mM $CaCl_2$, 2.5 mM benzamidine, 0.9 M ammonium sulfate, and 5.0 mM MES, pH 6.0, equilibrated against a reservoir of 5.0 mM MES, 1.0 mM $CaCl_2$, 2.5 mM benzamidine, and 1.8 M ammonium sulfate, pH 6.0. To remove benzamidine, crystals were transferred to buttons for dialysis against 2.8 M ammonium sulfate, 10 mM sodium phosphate, pH 6.5, and 2% DMSO. After 24 h, the buttons were transferred to

Table 1: Crystallographic Parameters for Bovine β-Trypsin Complexes

	ACPU	APPU	APPU (LT)
resolution (Å)	1.80	1.80	1.80
R_{merge}	0.11	0.11	0.14
observed reflections	201 510	191 406	105 428
unique reflections	28 730	27 448	19 267
% unique reflections	0.97	0.96	0.95
unit cell constants (Å)			
a	54.84	54.89	54.36
b	58.49	58.60	58.20
c	67.83	67.71	66.61
R-value	0.171	0.179	0.196
rms deviation of bond lengths from ideality (Å)	0.012	0.013	0.013
rms deviation of bond angles from ideality (deg)	2.64	2.73	2.82
no. of water molecules	97	82	165

0.6 mM of ACPU or APPU in the same solution. After soaking for 7−14 days, crystals of approximate size 0.4 × 0.4 × 0.7 mm were mounted in glass capillaries. For the LT trypsin-APPU data set, a crystal was subjected to shock cooling by immersion of the capillary into liquid nitrogen before transfer to a stream of low-temperature nitrogen gas.

X-ray intensity data were collected at 293 K (RT) or 113 K (LT) with a San Diego Multiwire Systems area detector (*17*) and an Enraf-Nonius cryostat (Model FR558S). CuKα radiation (1.5418 Å) was generated with a fine-focus Rigaku RU200 rotating anode operating at 100 mA and 46 kV.

Refinement of Trypsin-ACPU and Trypsin-APPU (*RT*). The refinement was initiated with the coordinates of benzamidine-inhibited trypsin (*10*) with all solvent and inhibitor molecules removed. The model was subjected to simulated-annealing followed by positional and displacement-factor refinement [XPLOR version 3.1; (*18*)]. A calcium ion was added to the conserved calcium-binding site (*19*) and the improved model was subjected to additional cycles of positional and displacement-factor refinement. At this stage, sum ($2|F_o| - |F_c|$) and difference ($|F_o| - |F_c|$) Fourier maps clearly showed inhibitor electron density in the S_1 pocket. A benzamidine molecule was docked into this electron density. The remainder of the inhibitor was gradually built into electron density as the refinement continued. The inhibitor was restrained by standard lengths and angles. Any parameters not available in the standard X-PLOR version 3.1 parameter files were obtained from CHARMm (*20*). Water molecules were added to corresponding sum and difference peaks in groups of 12 or fewer per refinement cycle. Except for doubly protonated His 57, all histidine residues were singly protonated at Nϵ2. The occupancies of O12 and ring C of APPU were maintained at zero because surrounding electron density was diffuse and poorly defined. Final crystallographic *R*-factors and other parameters are listed in Table 1.

Refinement of Trypsin-APPU (*LT*). The inhibitor from the RT trypsin-APPU structure was docked into LT electron density, with the occupancies of the O12 and ring C set to zero. After positional and displacement-factor refinement, water molecules from the RT structure were added in groups of 30 or fewer per cycle to corresponding sum and difference electron density peaks. After all possible waters from the RT structure were in place, additional waters and solvent molecules were added and refined in groups of 12 or less per refinement cycle.

Scheme 1

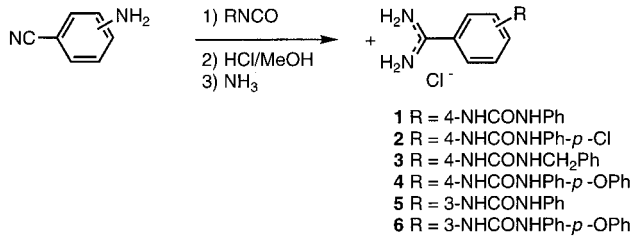

1 R = 4-NHCONHPh
2 R = 4-NHCONHPh-*p*-Cl
3 R = 4-NHCONHCH$_2$Ph
4 R = 4-NHCONHPh-*p*-OPh
5 R = 3-NHCONHPh
6 R = 3-NHCONHPh-*p*-OPh

Scheme 2

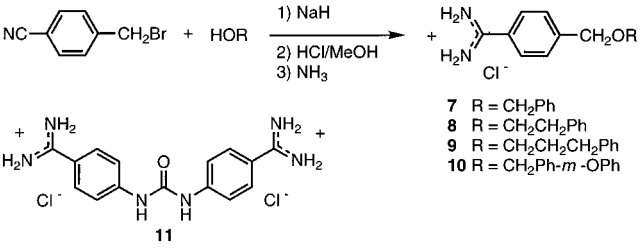

7 R = CH$_2$Ph
8 R = CH$_2$CH$_2$Ph
9 R = CH$_2$CH$_2$CH$_2$Ph
10 R = CH$_2$Ph-*m*-OPh

11

RESULTS

Synthesis Yields Novel Aryl Derivatives of Benzmidine. The urea-class inhibitors were synthesized by the general method depicted in Scheme 1. 4-Aminobenzonitrile reacted with the appropriate isocyanate to give the cyano-substituted phenylurea as a white solid. The cyano compounds were converted into the amidine derivatives using a modified Pinner reaction (*13*) that involved treatment with methanol/HCl to give the imidate ester, followed by refluxing in 2-propanol saturated with ammonia. The ether-class inhibitors were synthesized by Williamson's reaction (Scheme 2), which involves reaction of the appropriate alkoxide with *p*-cyanobenzylbromide. The Pinner reaction was used to convert the nitriles into amidines. The bis-amidino compound **11** was synthesized as previously described for the preparation of substituted 1,3-di(amidinophenyl)ureas (*21*). Refluxing 2 equiv of 4-aminobenzamidine with 1 equiv of urea in water gave the desired bis-amidine.

Compounds Demonstrate Competitive, Micromolar Inhibition of Five Trypsin-like Enzymes. The urea and ether derivatives of benzamidine described here all demonstrate competitive inhibition kinetics with the enzymes tested. The K_i values are in the micromolar range (Table 2). Overall, the inhibitors are more effective against bovine trypsin than against the other enzymes tested. For bovine trypsin, the lowest values (K_is ≈ 2−3 μM) were obtained with two extended aromatic compounds (**4**, **10**) and a bis-amidinophenyl compound (**11**). None of the compounds demonstrate potent inhibition of rat skin tryptase (K_is ≈ 40−200 μM); however, urea derivatives inhibit this enzyme 2−3-fold better than ether derivatives. The most effective inhibitor of rat skin tryptase (compound **6,** K_i = 38 μM) was the most effective inhibitor of human recombinant granzyme A (K_i = 8.0 μM). The lowest K_i values for the coagulation proteases human thrombin and human kallikrein were obtained with an ether-linked extended aromatic compound (**10**, K_i for thrombin = 2.9 μM, K_i for kallikrein = 28 μM). All other inhibitors showed only modest potency (K_is ≈ 50−300 μM) for these two enzymes.

Sulfate Can Modulate Potency of Trypsin Inhibitors. Several of the compounds introduced here demonstrate

Table 2: Inhibition Constants [K_i (μM)] for Bovine Trypsin, Human Thrombin, Rat Skin Tryptase, Human Recombinant Granzyme A, and Human Plasma Kallikrein

inhibitor	trypsin[a]	thrombin[b]	tryptase[c]	granzyme A[d]	kallikrein[e]
1	24 ± 0.9	173 ± 24	53 ± 15	34	62
2 (ACPU)	16 ± 2.8	210 ± 8.0	64 ± 6.9	35	189
3	34 ± 1.8	181 ± 18	70 ± 7.7	16	172
4 (APPU)	2.9 ± 0.1	NI[f]	NI[f]	90	54
5	43 ± 13	254 ± 36	66± 17	22	210
6	16 ± 3.0	51 ± 1.9	38 ± 5.9	8	NI[g]
7	9.6 ± 6.4	72 ± 8.0	203 ± 15	346	156
8	12 ± 3.4	127 ± 15	201 ± 58	68	132
9	11 ± 2.7	123 ± 11	168 ± 19	74	82
10	2.2 ± 0.9	2.9 ± 1.0	193 ± 21	108	28
11	3.2 ± 0.5	318 ± 28	75 ± 4.2	58	62

[a] In 0.1 M HEPES, 10 mM M $CaCl_2$, pH 7.5, and 9% DMSO. Values are averages, and uncertainties are 95% confidence limits determined using three substrate concentrations. [b] In 0.1 M HEPES, 0.5 M NaCl, 0.1% PEG 6000, pH 7.5, and 9% DMSO. Values are averages, and uncertainties are 95% confidence limits determined using three substrate concentrations. [c] In 0.1 M HEPES, pH 7.5, 10% glycerol, 10 μM heparin, and 3% DMSO. Values are averages, and uncertainties are 95% confidence limits determined using three substrate concentrations. [d] In 0.1 M HEPES, 10 mM $CaCl_2$, pH 7.5, and 9% DMSO. Values are determined using two substrate concentrations. [e] In 0.1 M HEPES, 0.5 M NaCl, pH 7.5, and 9% DMSO. Values are determined using two substrate concentrations. [f] No inhibition at inhibitor concentration up to 140 μM. [g] No inhibition at inhibitor concentrations up to 300 μM.

Table 3: Effect of Sulfate and pH on Inhibition Constants [K_i (μM)] of Benzamidine and ACPU with Bovine Trypsin[a]

	Benzamidine	ACPU
buffer + NaCl, pH 7.5[b]	77 ± 12	14 ± 1.3
buffer + Na_2SO_4, pH 7.5[c]	60 ± 4.0	10 ± 2.1
$K_{i,control}/K_{i,sulfate}$	1.3	1.4
buffer + NaCl, pH 6.0[d]	102 ± 13	33 ± 3.1
buffer + Na_2SO_4, pH 6.0[e]	74 ± 11	6.2 ± 1.8
$K_{i,control}/K_{i,sulfate}$	1.4	5.3
buffer + NaCl (2×), pH 6.0[f]	113 ± 16	53 ± 4.5
buffer + Na_2SO_4 (2×), pH 6.0[g]	100 ± 8.0	9.4 ± 0.3
$K_{i,control}/K_{i,sulfate}$	1.1	5.6

[a] Values are averages, and uncertainties are 95% confidence limits determined using three substrate concentrations. [b] In 0.1 M HEPES, 5 mM $CaCl_2$, 0.2 M NaCl, pH 7.5, and 9% DMSO. [c] In 0.1 M HEPES, 5 mM $CaCl_2$, 0.1 M Na_2SO_4, pH 7.5, and 9% DMSO. [d] In 0.1 M MES, 5 mM $CaCl_2$, 0.2 M NaCl, pH 6.0, and 9% DMSO. [e] In 0.1 M MES, 5 mM $CaCl_2$, 0.1 M Na_2SO_4, pH 6.0, and 9% DMSO. [f] In 0.1 M MES, 5 mM $CaCl_2$, 0.4 M NaCl, pH 6.0, and 9% DMSO. [g] In 0.1 M MES, 5 mM $CaCl_2$, 0.2 M Na_2SO_4, pH 6.0, and 9% DMSO.

sulfate mediated, pH-dependent reductions of K_i value when assayed with bovine trypsin. To control for effects of ionic strength, compounds were assayed in constant sodium concentration, either sodium sulfate (100 mM) or sodium chloride (200 mM; Table 3). The results indicate that sulfate ion-mediated reduction of the K_i value for ACPU is pH dependent. At high pH (7.5), the K_i value of ACPU is not dependent on sulfate. However, at low pH (6.0), the K_i value for ACPU is reduced 5.3-fold, from 33 to 6 μM, upon addition of sulfate. Error analysis indicates that the sulfate-mediated decrease of K_i of ACPU at pH 6.0 is statistically significant. Use of three substrate concentrations for each K_i measurement allows for calculation of confidence intervals for each K_i value (Table 3). The sulfate-ion mediated reduction of the K_i value for ACPU is limiting at high sulfate concentration. Doubling the sulfate concentration (from 100 to 200 mM) does not further reduce the K_i value (Table 3). Minimal sulfate ion-mediated reduction of the value K_i of ACPU was observed when the assay was carried out in buffer with lesser quantities of sulfate (25 mM, results not shown). Benzamidine shows only minimal reduction of K_i value upon addition of sulfate at high or low pH (1.3-fold reduction at pH 7.5, 1.4-fold reduction at pH 6.0).

Table 4: Effect of Sulfate on Inhibition Constants [K_i (μM)] for Bovine Trypsin at Low pH[a]

compd	control[b]	sulfate[c]	$K_{i,control}/K_{i,sulfate}$
B	102 ± 13	74 ± 11	1.4
1	66 ± 12	19 ± 0.7	3.5
2 (ACPU)	33 ± 3.1	6.2 ± 1.8	5.3
3	65 ± 9.5	35 ± 2.0	1.9
4 (APPU)	27 ± 0.5	13 ± 2.2	2.1
5	136 ± 9.4	124± 31	1.1
7	48 ± 4.8	34 ± 12	1.4
10	10 ± 0.6	8.6 ± 2.0	1.2
11	12 ± 0.7	1.8 ± 0.1	6.9

[a] Values are averages, and uncertainties are 95% confidence limits determined using three substrate concentrations. [b] In 0.1 M MES, 5 mM $CaCl_2$, 0.2 M NaCl, pH 6.0, and 9% DMSO. [c] In 0.1 M MES, 5 mM $CaCl_2$, 0.1 M Na_2SO_4, pH 6.0, and 9% DMSO.

Similarly, phosphate-mediated K_i reduction is observed for ACPU when tested against bovine trypsin in acidic conditions. The K_i value for ACPU was reduced from 33 ± 3.1 μM (control buffer) to 8.7 ± 2.7 mM (buffer + 100 μM Na_2HPO_4) at mildly acidic conditions (pH 6.0), a 3.8-fold decrease. Benzamidine was found to undergo K_i reduction similar to that found with sulfate (data not shown).

At low pH, ACPU and **11**, which are both para-substituted urea derivatives, show significant reduction of K_i values upon addition of sulfate (ACPU, 5.3; **11**, 6.9-fold; Table 4). Other derivatives show only slight reduction of K_i value. For several compounds, including benzamidine, two ether derivatives (**7** and **10**), a meta-substituted urea derivative (**5**), and two para-substituted urea derivatives (APPU and **3**), reduction of K_i value is minimal (1−2-fold). Another para-substituted urea derivative (**1**) shows an intermediate reduction of K_i value.

For human thrombin, K_i values for one compound (**1**) were determined in buffer with excess sulfate ion and control buffer. At pH 6.0, the K_i values of **1** were 127 ± 4.9 μM (control buffer) and 103 ± 4.0 μM (100 mM Na_2SO_4). The minimal sulfate-mediated reduction of K_i value observed for this compound (1.2-fold) was similar to that seen for benzamidine (results not shown). ACPU, APPU, and compound **11** showed no inhibition of thrombin at pH 6.0 up to their limits of solubility (140, 400, and 850 μM, respectively).

Room-temperature X-ray structures of bovine β-trypsin complexes with ACPU and APPU and a low-temperature structure of the APPU complex were determined. In each inhibited complex, the protein is well-defined by electron density, with the exception of Ser 146 and Ser 147 in the autolysis loop (*16*) and the soft main-chain residues Asn 115 and Ser 116 (*10*). The structure of β-trypsin, including the active-site region, is similar in all three of the inhibitor complexes.

Structure of the Trypsin−ACPU Complex Reveals ACPU and a nearby Sulfate Ion within the Active Site. The amidino moiety of ACPU inserts into the S_1 pocket with position (Figure 2A) and interactions very similar to those of benzamidine (*10*). As in trypsin complexes with other

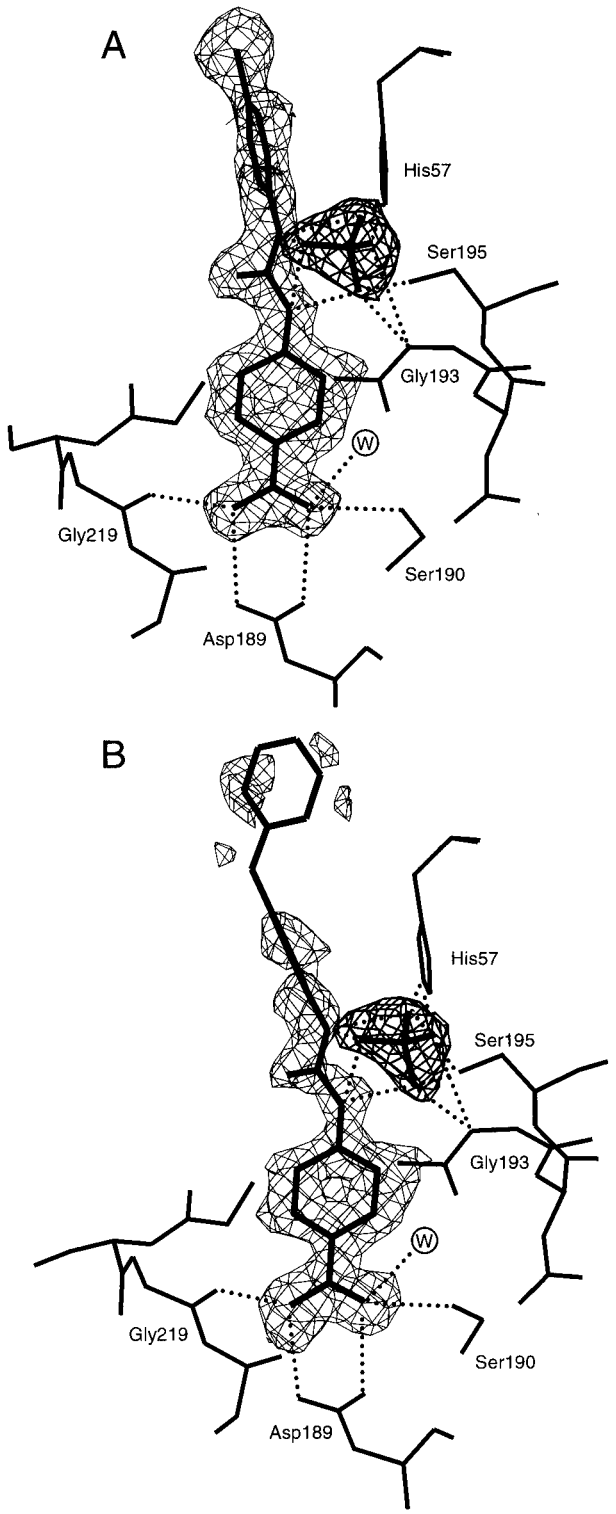

FIGURE 2: Fourier difference ($F_o - F_c$) maps of ternary inhibitor/sulfate/trypsin complexes. (A) ACPU and (B) and APPU at low temperature. Before map computation the coordinates of the inhibitor and adjacent sulfate ion were omitted. Maps are contoured at 2.0σ and are drawn with thin lines surrounding inhibitor and thick lines surrounding sulfate ion. Bonds are grouped by width with inhibitor = sulfate > protein. Hydrogen bonds are indicated by dotted lines. A water molecule is denoted by an enclosed W.

amidinophenyl- and arginine-based inhibitors (*22, 10, 23, 24*), the amidino group forms two hydrogen bonds with the carboxylate group of Asp 189 and with Gly 219 O, Ser 190 Oγ, and a buried water molecule (Figures 2 and 3, and Table 5). The interaction of amidino N1′ with the buried water molecule and Ser 190 Oγ is via a three-centered ("bifurcated") hydrogen bond. A single proton of the amidino group is shared by lone pairs of both the water molecule and Ser 190 Oγ.

The carbonyl bond (C8 → O8) of ACPU is directed away from the protein and into the solvent channel such that O8 does not form hydrogen bonds with the protein. Ring B lacks van der Waals contacts with trypsin and is located approximately 3.8 Å from the imidazole ring of His 57. The chlorine substituent on ring B projects into the solvent channel. This lack of interaction of ring B with trypsin suggests that this class of inhibitor could be significantly improved by appropriate chemical modification of functional groups to achieve favorable interaction with binding sites outside of the primary specificity pocket.

A feature unique to these structures not seen in previously published serine protease-inhibited structures is the linkage of the inhibitor (ACPU) to the protein via a complex network of hydrogen bonds involving a well-ordered sulfate ion (described below).

Two Structures of the Trypsin−APPU Complex Reveal Conformational Heterogeneity within the Active Site. The amidinophenyl and urea moieties of APPU are well-defined by electron density maps (Figure 2B). Interactions between atoms of the amidinophenyl moiety of APPU and trypsin are similar to those seen in the ACPU−trypsin complex. In both RT and LT structures, the inhibitor amides of APPU are bound to protein atoms via a hydrogen-bonding network involving a well-ordered sulfate ion, similar to that seen in the ACPU-trypsin structure (described below). The LT electron density maps are sharper and more detailed than the RT maps (not shown). The positions of the phenylphenoxy portion (O12 and rings B and C) are unresolved. At both RT and LT, the electron density maps of this portion of the molecule are diffuse. Ring B, whose position is estimated from the limited electron density in the maps, appears to be inserted into the S_2 pocket, occupying a position similar to that of the piperidine ring in the NAPAP−trypsin complex (*25*). A broad range of possible positions occupied by ring C can be estimated by possible rotations about the C12−O12 and O12−C15 bonds. To avoid phase errors, the occupancy of ring C was maintained at zero during refinement and map calculations.

Modeling of ACPU and APPU into Human Thrombin Reveals Unfavorable Contacts. ACPU fits into the active site of thrombin with the exception of unfavorable contacts of the chlorine atom (Figure 4). ACPU was docked into human α-thrombin by optimally superimposing residues of the catalytic triad and Asp 189. The thrombin structure employed was the complex of PPACK bound to human α-thrombin (*26*). As expected, contacts of the amidinophenyl and urea moieties with thrombin are virtually identical to those with trypsin. The sulfate ion similarly shows identical interactions with the two enzymes. The main difference between the S_1 pockets of trypsin and thrombin is the replacement of Ser 190 of trypsin with Ala 190 of thrombin. This switch makes the thrombin pocket slightly less polar and precludes a hydrogen bond between Ser 190 of thrombin and N1′ of the inhibitor. Ring B of ACPU forms unfavorable contacts with Tyr 60A of thrombin (Figure 4). Distances between atoms are in the range 1.7−2.5 Å. The unfavorable contacts of Tyr 60A with APPU are also severe

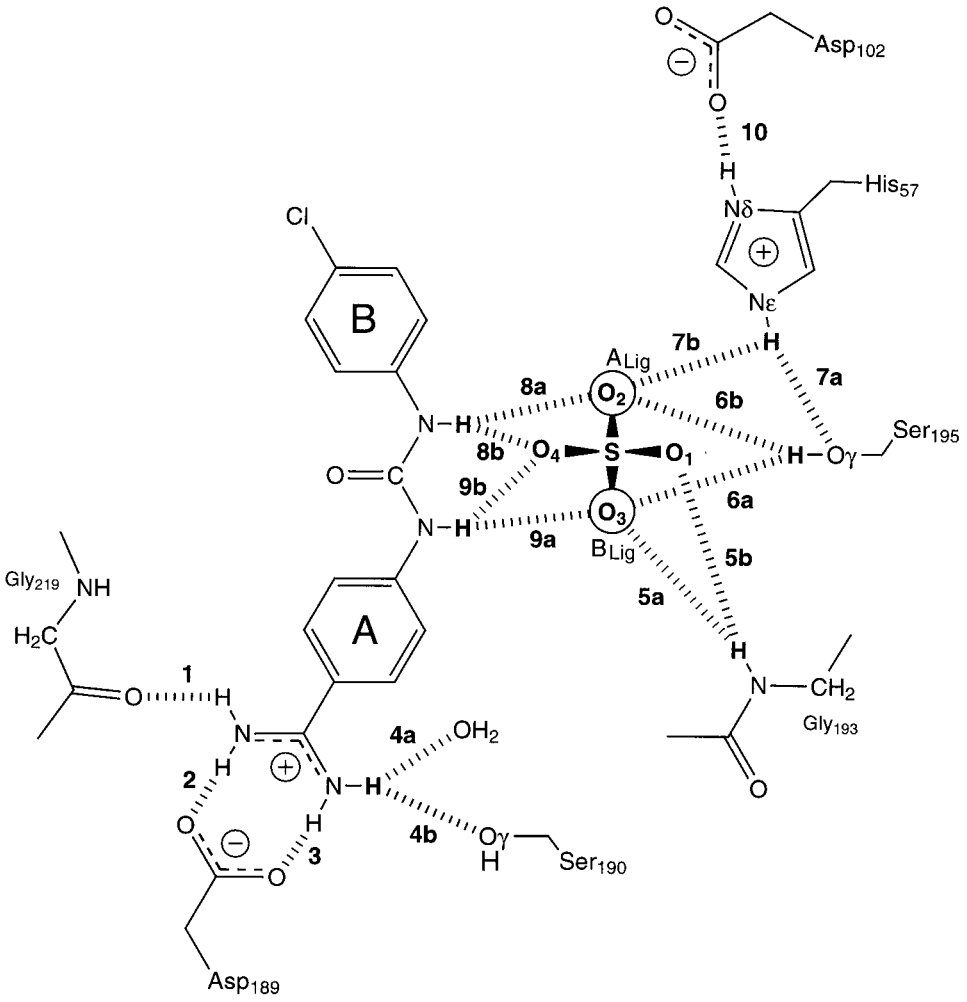

FIGURE 3: Schematic diagram of hydrogen bonding interactions in the trypsin−ACPU complex. Hydrogen bonds are numbered. Three center hydrogen bonds are designated by lowercase letters a and b. Hydrogen atoms involved in three center hydrogen bonds are bold. Conserved noncovalent oxyanion positions (A_{Lig} and B_{Lig}) are indicated.

Table 5: Hydrogen-Bonding Distances (Å) and Angles (deg) in Bovine β-Trypsin Complexes[a]

			ACPU (RT)		APPU (RT)		APPU (LT)	
HB no.	atom 1	atom 2	dist	angle	dist	angle	dist	angle
1	Inh N1	Gly 219 O	2.9	157	2.8	159	2.9	154
2	Inh N1	Asp 189 Oδ1	2.9	165	2.9	168	2.8	165
3	Inh N1′	Asp 189 Oδ2	2.9	172	2.8	176	2.8	172
4a	Inh N1′	Wat 512 O	3.0	126	2.9	133	3.0	129
4b	Inh N1′	Ser 190 Oγ	2.7	121	2.7	119	2.6	124
5a	Gly 193 N	SO_4^{2-} O3	3.1	148	3.1	147	3.2	143
5b	Gly 193 N	SO_4^{2-} O1	3.3	150	3.5	153	3.2	156
6a	Ser 195 Oγ	SO_4^{2-} O3	2.7	144	2.7	142	2.8	149
6b	Ser 195 Oγ	SO_4^{2-} O2	3.0	145	3.2	147	3.0	142
7a	His 57 Nϵ2	Ser 195 Oγ	2.9	124	3.1	125	3.0	119
7b	His 57 Nϵ2	SO_4^{2-} O2	2.8	143	2.8	145	2.8	149
8a	Inh N9	SO_4^{2-} O2	3.0	140	3.1	145	2.9	143
8b	Inh N9	SO_4^{2-} O4	2.9	150	3.0	152	2.9	143
9a	Inh N5	SO_4^{2-} O3	3.0	175	3.0	169	2.9	163
9b	Inh N5	SO_4^{2-} O4	(3.5)[b]	132	(3.4)[b]	134	(3.5)[b]	138

[a] The hydrogen bond numbering scheme is illustrated in Figure 3. Three-centered hydrogen bonds are designated by letters a and b. Distances are from heteroatom to heteroatom (d[A···B]). Angles are from heteroatom to hydrogen atom to heteroatom (a[A···H−B]). Hydrogen atom positions were determined by geometry, with N−H distances of 1.0 Å, C−N−H angles of 120°, and H coplanar with C and N. [b] Distance approaches hydrogen bond length cutoff.

(not shown), consistent with poor inhibitory potency of APPU for thrombin (Table 2).

Sulfate Ions Mediate a Multiple-Centered Hydrogen-Bonding Network within the Active Site. Trypsin is linked to a sulfate ion that is in turn linked to ACPU or APPU (Figures 2 and 3) by intricate networks of three-centered hydrogen bonds. By the nomenclature of Taylor and coworkers (*27*), a proton in a three-centered hydrogen bond interacts with two acceptor atoms. Each of three-centered hydrogen bonds described here (Table 5) is consistent with

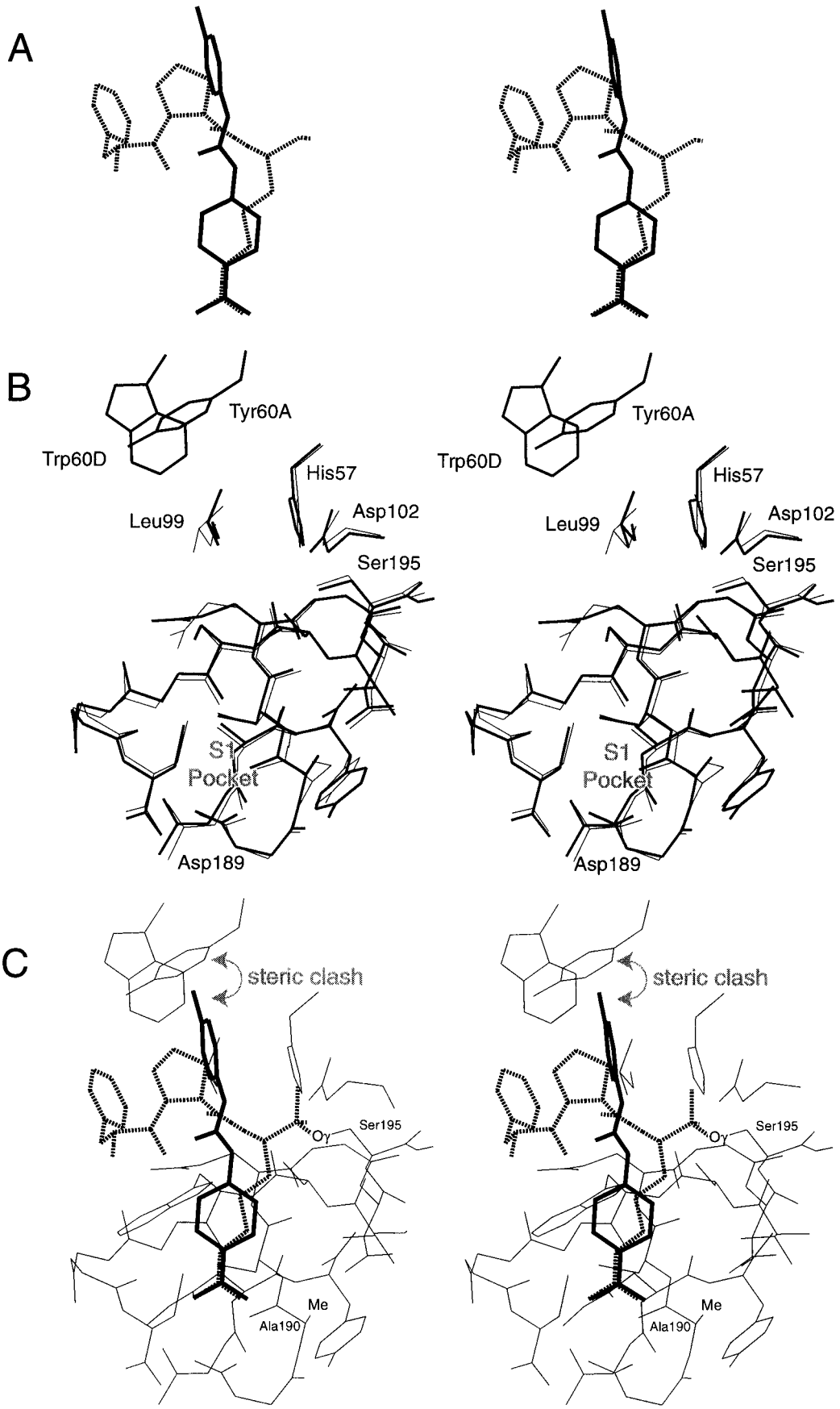

FIGURE 4: (A) Stereo drawing of ACPU (solid lines) superimposed on PPACK (dashed lines), (B) the active site region of trypsin from the ACPU complex (thin lines), superimposed on the active-site region of thrombin from the PPACK inhibited complex. (C) Same as panel B with ACPU and PPACK included. All superimpositions were achieved by minimizing deviations of atoms in trypsin/thrombin residues Ser 195, Asp 102, His 57, and Asp 189 (rms deviation 0.31 Å). The thrombin−PPACK complex is PDB 1PPB (*26*).

Table 6: Serine Protease Complexes with Noncovalent Oxyanions

code	protein	oxyanion ligand	other ligands[a]	temp of coll	res (Å)	pH[b]	ref
ACPU	bovine trypsin	SO_4^{2-}	ACPU	RT	1.80	6.5	this paper
APPU	bovine trypsin	SO_4^{2-}	APPU	RT, −160 °C	1.80	6.5	this paper
2ALP	α-lytic protease	SO_4^{2-}		RT	1.70	6.1	*32*
1BIT	salmon typsin	SO_4^{2-}	Benzamidine	RT	1.83	5.0	*46*
1ELA	porcine elastase	CH_3COO^-	Inh[c]	RT	1.80	5.0	*47*
1ESA	porcine elastase	SO_4^{2-}		−45 °C	1.65	6.7	*48*
3EST	porcine elastase	SO_4^{2-}		RT	1.70	6.1	*49*
1GBJ	α-lytic protease	SO_4^{2-}		RT	2.00	8.0	*50*
1TAL	α-lytic protease	SO_4^{2-}		−120 °C	1.50	7.5	*51*
1TLD	bovine tryspin	SO_4^{2-}	Benzamidine	RT	1.60	5.3	*30*

[a] Other ligands in the active site. [b] Refers to pH of either crystallization or soaking solution. [c] Inhibitor: trifluoroacetyl-L-lysyl-L-prolyl-P−isopropylanilide (*47*).

the geometric criteria of Taylor and co-workers (*27*). With five hydrogen bond donors involved in a total of 10 hydrogen bonds, the interactions of the sulfate ion deviate significantly from statistical expectations. The norm for hydrogen bonding is two centers. In a random set of N−H···O hydrogen bonds, only 20% are three centered (*27*). If the set is limited to intermolecular hydrogen bonds, the three-centered frequency falls to less than 10%. In the trypsin complexes described here, the sulfate ion forms the following hydrogen bonds with protein and inhibitor. (1) The hydrogen on N of Gly 193 forms three-centered hydrogen bonds to sulfate atoms O3 (hydrogen bond 5a in Figure 3 and Table 5) and O1 (hydrogen bond 5b). (2) The hydrogen on Oγ of Ser 195 forms three-centered hydrogen bonds to sulfate atoms O3 (6a) and O2 (6b). (3) The hydrogen on Nϵ2 of His 57 forms three-centered hydrogen bonds to Ser 195 Oγ (7a) and sulfate O2 (7b). (4) The hydrogen on N-9 of the inhibitor forms three-center hydrogen bonds to sulfate atoms O2 (8a) and O4 (8b). (5) The hydrogen on N-5 of the inhibitor appears to form three-centered hydrogen bonds to sulfate atoms O3 (9a) and O4 (9b). The N-5 atom is within hydrogen-bonding distance of sulfate O3 but is near our hydrogen bond cutoff distance (3.4 Å) from O4 (Table 5). Therefore, the interactions of N-5 are difficult to classify and may be either two-centered or weak three-centered hydrogen bonds. High proportions of multiple-center bonds have been observed previously in small-molecule crystal structures with deficiencies of proton donors relative to acceptors (*28*).

Oxyanion Positions are Conserved. Two of the four sulfate oxyanion atoms seen in the ACPU and APPU−trypsin complex structures presented here occupy highly conserved noncovalent oxyanion-binding sites. We examined the structures of serine proteases with oxyanion ligands bound noncovalently in the active site available from the Protein Data Bank (*29*). Structures were screened by the following criteria: (i) resolution at or below 2.0 Å, (ii) reasonable internal geometry of the ligand, (iii) reasonable occupancy (greater than 0.5) of ligand atoms, and (iv) single occupancy of ligand atoms and residues in the active site. Using these criteria, eight coordinate sets of serine proteases with either a sulfate or acetate ion residing in the active site were utilized (Table 6). All coordinate sets were regarded as unique due to differences in protease type, absence or presence of inhibitors, temperature of data collection (RT or frozen), or laboratory of origin. These 10 coordinate sets (ligands = nine sulfate and one acetate ion, Table 6), including the trypsin−ACPU and trypsin−APPU (LT) complexes, were superimposed upon a template structure [PDB code 1TLD (*30*)] by minimizing deviations in position of atoms His 57 Nϵ2, Gly 193 N, and Gly 195 N. Serine 195 Oγ was not used in the superimposition because of the relatively high variation in the position of this atom among crystal structures.

Table 7: Distances between Pairs of Oxyanion Ligand and Tetrahedral Intermediate Average Oxyanion Positions

	distance (Å)	sum of 95% confidence limits (Å)
$A_{Lig}-A_{Tet}$	0.69	0.28
$B_{Lig}-B_{Tet}$	0.79	0.34
$A_{Lig}-B_{Tet}$	2.8	0.29
$B_{Lig}-A_{Tet}$	1.7	0.24
$A_{Lig}-B_{Lig}$	2.3	0.22
$A_{Tet}-B_{Tet}$	2.4	0.31

Superimposition of noncovalent oxyanion trypsin complexes reveals that certain oxyanions occupy conserved positions within the active site. Two distinct groups of oxyanion atoms could be clearly defined. Each group of 10 oxyanion atoms (one atom from each of the 10 coordinate sets) was found to be localized within a characteristic region in space separate from the other group well beyond the 95% confidence level (Table 7). The consensus sites, the average of 10 positions, are termed here position A_{Lig} and position B_{Lig} (Figure 5). The O2 atoms of sulfate ions in the ACPU and APPU complexes occupy the A_{Lig} site. The O3 atoms occupy the B_{Lig} site. In sum, 10 oxyanion atoms are closely sequestered around positions A_{Lig} (rms deviation 0.56 Å) and B_{Lig} (rms deviation 0.52 Å). Additional oxyanion atoms not belonging to groups A_{Lig} and B_{Lig} could not be sequestered clearly into two groups. These atoms occupy more random positions.

Hydrogen bonds of oxyanions in groups A_{Lig} and B_{Lig} with active-site atoms show highly conserved distance and geometry (Table 8). Oxyanions in position A_{Lig} form hydrogen bonds to both His 57 imide and Ser 195 hydroxyl groups. Those in position B_{Lig} form hydrogen bonds to Gly 193 N amide and Ser 195 hydroxyl groups. Hydrogen bond geometry of oxyanions atoms (lone-pair donors) relative to protein heteroatoms (proton donors) and other atoms is reasonable (Table 8). For hydrogen bonds involving amide or imide proton donors, geometry is optimized when acceptor atom, proton, donor atom, and backbone atoms line in the same plane. For the hydrogen bond linking His 57 Nϵ2 imides to A_{Lig} atoms, A_{Lig} atoms lie nearly in the same plane as His 57 Nϵ2, Cδ2, and Cϵ1 atoms in the structures surveyed. For the hydrogen bond linking Gly 193 N amides to B_{Lig} atoms, B_{Lig} atoms lie nearly in the same plane Gly 193 N, Cα, and C atoms.

A_{Lig} and B_{Lig} oxyanions, along with His 57 Nϵ2, Ser 195 Oγ, and Gly 193 N atoms, form vertexes of a pair of triangles

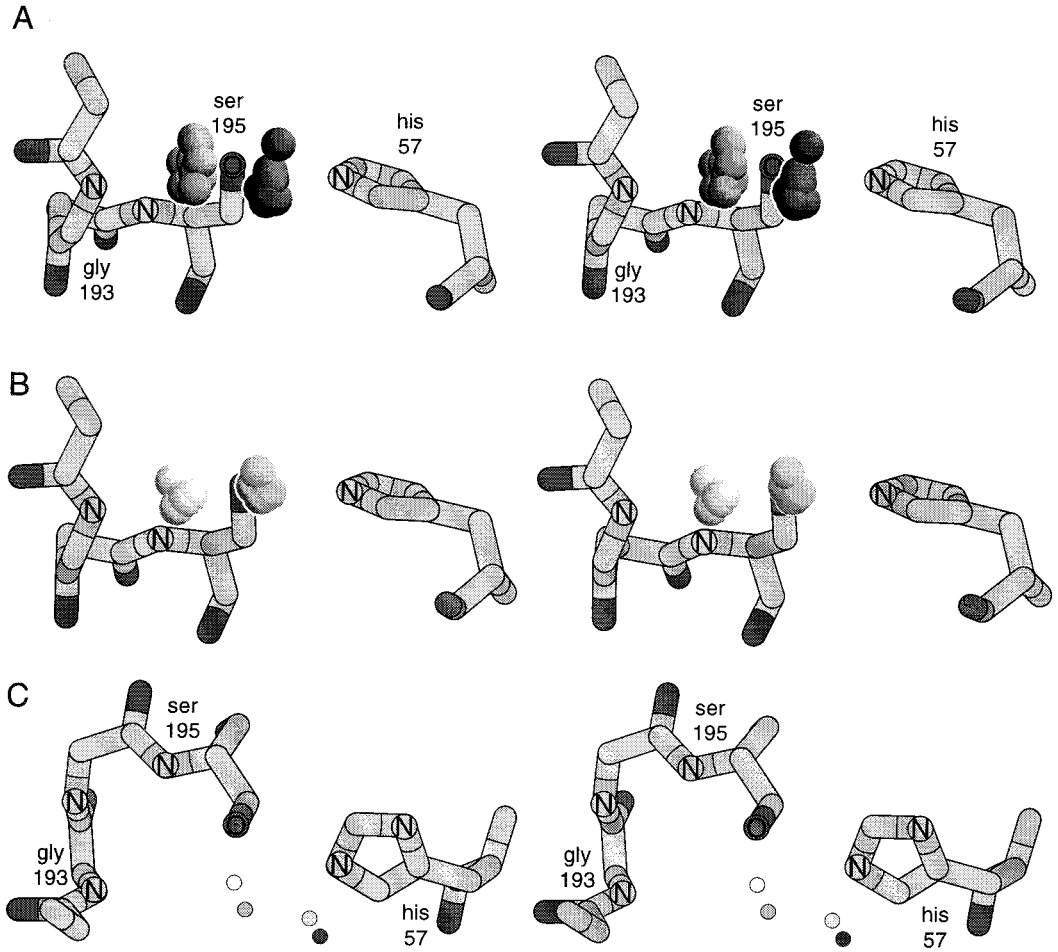

FIGURE 5: Active-site region of trypsin. Oxyanions are shaded in the order $A_{lig\ (dark)} > B_{Lig} > A_{Tet} > B_{Tet}$ (light). (A) Noncovalent oxyanions within A_{Lig} and B_{Lig} sites; (B) covalent oxyanions within the A_{Tet} and B_{Tet} positions; and (C) average A_{Lig}, B_{Lig}, A_{Tet}, and B_{Tet} positions. This panel is rotated 90° relative to the other panels. Conserved oxyanion positions are shown relative to active-site residues of structure 1TLD (*30*) in all panels. Superimpositions were achieved by minimizing deviations of His 57 Nϵ2, Gly 193 N, and Ser 195 N from serine protease complexes with noncovalent oxyanions (10 structures, rms deviation 0.069 Å) or tetrahedral intermediate analogues (five structures, rms deviation 0.053 Å).

Table 8: Hydrogen-Bonding Distances (Å) and Angles (deg) in Noncovalent and Covalent Oxyanion Complexes with Serine Proteases[a]

	A_{Lig}	B_{Lig}	A_{Tet}	B_{tet}
		distance		
$N\epsilon2_{57}$	2.9 ± 0.07	*b*	2.8 ± 0.16	*b*
$O\gamma_{195}$	3.3 ± 0.12	2.7 ± 0.07	2.3 ± 0.04	2.4 ± 0.02
N_{193}	*b*	2.8 ± 0.11	*b*	2.8 ± 0.14
N_{194}	*b*	*b*	*b*	3.5 ± 0.17
N_{195}	*b*	3.9 ± 0.17	*b*	3.0 ± 0.09
		Angles		
$C\epsilon1_{57}-N\epsilon2_{57}$	149 ± 3.2	*b*	137 ± 5.2	*b*
$C\beta195-O\gamma_{195}$	94 ± 5.9	101 ± 5.8	109 ± 8.3	99 ± 6.3
$C\alpha193-N_{193}$	*b*	123 ± 7.2	*b*	113 ± 6.6
$C\alpha194-N_{194}$	*b*	*b*	*b*	118 ± 2.1
$C\alpha195-N_{195}$	*b*	92 ± 2.0	*b*	98 ± 3.2

[a] Values are averages of distances and angles of the superimposed coordinate sets. Uncertainties are expressed as 95% confidence limits. [b] Distance is greater than hydrogen bond threshold of 4.0 Å.

with nearly symmetric dimensions in the active sites of the superimposed structures (Figure 6). After superimposition, His 57 Nϵ2, Ser 195 Oγ, and Gly 193 N atoms, along with oxyanions A_{Lig} and B_{Lig}, were found to have minimal deviations from a similar plane (average rms deviation 0.53 Å). Within this plane, A_{Lig} oxyanions, His 57 Nϵ2, and Ser 195 Oγ atoms mark the vertexes of a nearly equilateral

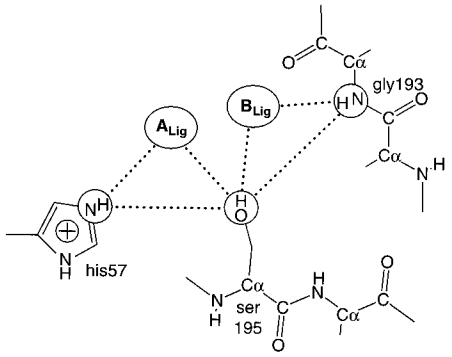

FIGURE 6: Schematic diagram of A_{Lig} and B_{Lig} positions relative to active-site residues of bovine trypsin. The triangular relationships proton donor and acceptor atoms are shown.

triangle. The sides of this triangle ($N\epsilon2_{57}-A_{Lig}$, 2.9 Å ± 0.07 Å; $A_{Lig}-O\gamma_{195}$, 3.3 Å ± 0.12 Å; $O\gamma_{195}-N\epsilon2_{57}$, 3.1 Å ± 0.13 Å), average 3.1 Å while the angles within the triangle ($\angle O\gamma_{195}-N\epsilon2_{57}-A_{Lig}$, 66 ± 1.7°; $\angle N\epsilon2_{57}-A_{Lig}-O\gamma_{195}$, 60 ± 2.4°; $\angle A_{Lig}-O\gamma_{195}-N\epsilon2_{57}$, 54 ± 2.7°) are all nearly 60° (Table 9). B_{Lig} oxyanions form one vertex of another triangle with other vertexes marked by Gly 193 N and Ser 195 Oγ atoms. Hydrogen bonds from B_{Lig} oxyanions to these atoms are of nearly equal length ($N_{193}-B_{Lig}$ = 2.8 Å ± 0.11 Å; $B_{Lig}-O\gamma_{195}$ = 2.7 Å ± 0.07 Å), with nearly identical angles

Table 9: Distances (Å) and Angles (deg) between Atoms in the Active Sites of 10 Oxyanion Ligand Serine Protease Complexes[a]

distance		angle	
$O\gamma_{195}-N\epsilon2_{57}$	3.1 ± 0.13	$N\epsilon2_{57}-A_{Lig}-O\gamma_{195}$	60 ± 2.4
$N\epsilon2_{57}-A_{Lig}$	2.9 ± 0.07	$A_{Lig}-O\gamma_{195}-N\epsilon2_{57}$	54 ± 2.7
$A_{Lig}-O\gamma_{195}$	3.3 ± 0.12	$O\gamma_{195}-N\epsilon2_{57}-A_{Lig}$	66 ± 1.7
$O\gamma_{195}-N_{193}$	4.8 ± 0.16	$O\gamma_{195}-B_{Lig}-N_{193}$	121 ± 7.1
$N_{193}-B_{Lig}$	2.8 ± 0.11	$N_{193}-O\gamma_{195}-B_{Lig}$	30 ± 4.1
$B_{Lig}-O\gamma_{195}$	2.4 ± 0.07	$B_{Lig}-N_{193}-O\gamma_{195}$	29 ± 3.2

[a] Values are averages from superimposed coordinate sets. Uncertainties are 95% confidence limits.

Table 10: Structures of Tetrahedral Intermediate Analog−Serine Protease Complexes

PDB code	protein	type of adduct	res (Å)	ref
1BTZ	bovine trypsin	boronic acid	1.80	52
1LHC	human thrombin	boronic acid	1.80	53
1P01	α-lytic protease	boronic acid	1.70	54
3VGC	chymotrypsin	boronic acid	1.83	55
1MAX	bovine trypsin	phosponate	1.80	56

($\angle N_{193}-O\gamma_{195}-B_{Lig} = 30 \pm 4.1°$; $\angle B_{Lig}-N_{193}-O\gamma_{195} = 29 \pm 3.2°$). The angle of the vertex formed by B_{Lig} oxyanions ($\angle O\gamma_{195}-B_{Lig}-N_{193} = 121 \pm 7.1°$) is much larger than the other two vertexes.

Oxyanion Positions of Tetrahedral Intermediates Differ from Noncovalent Oxyanion Positions. The oxyanion positions A_{Lig} and B_{Lig}, which are binding sites for noncovalent oxyanions, are distinct from the positions of covalently linked oxyanions of tetrahedral intermediate analogues. The distinction is statistically significant well beyond 95% confidence levels. We examined structures available from the PDB of serine proteases covalently bound to tetrahedral intermediate analogues. These structures were selected using criteria similar to those used for noncovalent oxyanion complexes, with the additional requirement than an oxyanion atom must be within hydrogen bonding distance (<3.4 Å) to the N atom of the amide of either residue 193, 194, or 195 (residues that line the oxyanion hole). Five serine proteases covalently linked with tetrahedral intermediate analogues (four boronic acid and one phosphonate) were selected with these criteria (Table 10). These covalent complexes were superimposed upon the reference structure [*1TLD* (*30*)] used for the noncovalent superimpositions and also by minimizing deviations of atoms His 57 Nϵ2, Gly 193 N, and Gly 195 N. As observed for noncovalent complexes, two groups of covalent oxyanion atoms (A_{Tet} and B_{Tet}) are clearly defined. Each each group of five atoms contains a single oxyanion atom from each tetrahedral intermediate protease complex. The average of each group of oxyanions defines positions A_{Tet} and B_{Tet} (Figure 5). The A_{Tet} and B_{Tet} positions are different from the A_{Lig} and B_{Lig} well beyond 95% confidence limits (Table 7). Positions of oxyanions within the A_{Lig}, B_{Lig}, A_{Tet}, and B_{Tet} positions and the catalytic and stabilizing residues of the active site of a reference structure [1TLD (*30*)] are visualized in Figure 5.

DISCUSSION

We have synthesized a novel series of benzamidine-based aryl protease inhibitors and have determined their inhibitory potencies for five trypsin-like proteases. In addition, we have determined three-dimensional X-ray structures of two of these inhibitors (ACPU and APPU; Figure 1) in complexes with trypsin. The three-dimensional structures indicate that the inhibitors interact within the S_1 pocket as intended, but fail to engage in direct and specific interactions with other regions of the protease active site. The lack of non-S_1 interactions is indicated in part by configurational disorder of the extended portions of APPU (O12 and rings B and C).

Although the inhibitors do not engage in direct and specific interactions outside the S1 pocket, they do form intimate *indirect* contacts with the proteases. These indirect interactions are mediated by sulfate ions and are pH switchable. Sulfate ions within the active site link protein to inhibitor in each three-dimensional structure (Figures 2 and 3, and Table 5). The sulfate ions act as virtual functional groups of the proteases. The hydrogen-bonding network linking sulfate ion to inhibitor and protease is comprised primarily of multiple-centered hydrogen bonds, where a single proton is donated to two or three hydrogen bond acceptors. The frequency of these multiple-centered hydrogen bonds between ligand and protease may indicate a mechanistic role during peptide hydrolysis. The advantage of multiple-centered over conventional hydrogen bonds is that each component interaction is relatively weak, allowing for a featureless energy surface during chemical transformation (*31*). Intermediates stabilized by multiple-centered hydrogen bonds would give lower activation energies than if disruption of one hydrogen bond is required before formation of another.

Two Distinct Noncovalent Oxyanion-Binding Positions Are Highly Conserved across at Least Two Serine Protease Classes. Superimposition of serine protease structures bound to small mobile oxyanions has allowed us to map out noncovalent oxyanion-binding sites (positions A_{Lig} and B_{Lig}, Figure 5). Small ligands such as sulfate and acetate have translational and rotational freedom and occupy positions of local minimum free energy. The conservation of oxyanion positions within the A_{Lig} and B_{Lig} sites is revealed by superimposition of 10 high-resolution serine protease structures (eight from the PDB and two described here) containing noncovalently bound oxyanions within their active sites (Table 6). In each of these 10 protease complexes, the A_{Lig} and B_{Lig} positions are occupied by oxyanions. In the structures described here, the O2 atoms of the sulfate ions occupy position A_{Lig}. The O3 atoms occupy position B_{Lig}. The positions appear to accept a variety of oxyanions, for example, from acetate (PDB code 1ELA). Our kinetic data suggest that phosphate oxyanions can also occupy the A_{Lig} and B_{Lig} positions.

The high conservation of oxyanion positions is indicated by small deviations from the A_{Lig} and B_{Lig} sites, which are the average positions for each group (Figure 5). Each group shows rms deviations from average position of around 0.5 Å, a value comparable to the rms deviations of Cα positions of conserved proteases (*32*−*34*). This conservation of noncovalently bound oxyanion positions is remarkable considering that the 10 superimposed structures are from two different protease specificity classes.

The Positions of Noncovalent Oxyanions Are Distinct from the Positions of Covalent Oxyanions. Tetrahedral intermediate oxyanions, which are covalently linked to the protease, occupy two highly conserved positions (positions A_{Tet} and

B_{Tet}). Five high-resolution structures of serine proteases in complexes with tetrahedral intermediate analogues (Table 10) were superimposed on the same reference structure (PDB code 1TLD) used for superimposition of the noncovalent oxyanion complexes. Two groups of covalent oxyanions are clearly apparent from the superimposition (Figure 5). The average positions of the two covalent groups are termed A_{Tet} and B_{Tet}. These covalent oxyanion positions differ from noncovalent oxyanion positions (A_{Lig} and B_{Lig}). The differences are statistically significant. The pairwise distances between pairs of four oxyanion positions (A_{Tet}, B_{Tet}, A_{Lig}, and B_{Lig}) are greater than the sums of the 95% confidence limits for each pair (Table 7).

Noncovalent Oxyanion Positions Fall outside the "Oxyanion Hole". Tetrahedral intermediates and transition states are thought to be stabilized by specific interactions within the oxyanion hole. In fact, covalent oxyanions in position B_{Tet} clearly do occupy the oxyanion hole and form hydrogen bonds of good geometry to protons on Gly 193 N and Ser 195 N and interact more weakly with Asp 194 N (Table 8). The B_{Lig} position is close to the oxyanion hole and is within hydrogen-bonding distance of the N atom of Gly 193. However, the B_{Lig} position is too far from the center of the hole to form hydrogen bonds to either Ser 195 N or Asp 194 N atoms. These two oxyanion positions (B_{Lig} and B_{Tet}) differ in position by less than 1 Å (0.79 Å). Yet, this difference in position between B_{Lig} and B_{Tet} results in significant differences in the interactions of noncovalent and covalent oxyanions with the protease. As shown in Table 8, noncovalent oxyanions engage in fewer stabilizing hydrogen-bonding interactions than covalent oxyanions.

Why do noncovalent oxyanions not enter the oxyanion hole? The oxyanion hole is simply too small to allow entry. Examination of the geometry of the oxyanion hole reveals that entry even by a water molecule or a hydronium ion is prohibited by unfavorable steric contacts with at least one atom lining the hole (atoms of resides Gly 193, Asp 194, and Ser 195). This steric repulsion hypothesis is supported by the vacancy of the oxyanion hole throughout a series of serine proteases that are not bound by covalent tetrahedral intermediate analogues [solved to better than 2.0 Å resolution; PDB codes 3PTB (*10*), 1DPO (*35*), 4CHA (*36*), 5CHA (*37*), 1ST3 (*38*), 1ELT (*39*)]. Neither water (concentration 55 M) nor hydronium ion (up to 1 mM) enters the oxyanion holes of these proteases.

How do covalently bound oxyanions gain entry into the oxyanion hole? Upon formation of a tetrahedral intermediate and entry into the oxyanion hole, a short repulsive contact is established between the oxyanion and the Oγ of Ser 195 ($B_{Tet}-O\gamma_{195}$, 2.4 Å ± 0.02 Å, Table 8). The unfavorable free energy of this short contact is compensated predominantly by the favorable free energy of covalent bond formation, allowing entry. In the absence of a covalent bond, the repulsive interaction dominates, blocking entry. In sum, a "thermodynamic gate" controls access to the oxyanion hole.

Catalytic Residue His 57 Is Doubly Protonated. In the complexes analyzed here, the van der Waals surfaces of oxyanions in the A_{Lig} position penetrate the surfaces of the nitrogen atoms of the Nϵ2 of His 57 ($N\epsilon2_{57}-A_{Lig}$ distance is 2.9 Å ± 0.07 Å; Table 8). These close contacts would be favorable and likely to occur with high frequency only if the Nϵ2 of His 57 were protonated. Deprotonation of the Nϵ2 of His 57 would cause the interaction to be energetically unfavorable. The short $N\epsilon2_{57}-A_{Lig}$ contact and the extreme conservation of the distance ($\sigma = 0.11$ Å), suggests that the Nϵ2 of His 57 is protonated [as is Nδ1 of the same histidine (40, 41)] in each of these noncovalent oxyanion complexes. Indeed most of the noncovalent oxyanion protease complexes used in this analysis were determined from crystals grown or soaked at a relatively acidic pH (Table 6), making protonation of the His 57 Nϵ2 imide in these structures reasonable.

Sulfate Ions Link Inhibitors to Protonated Proteases. Our kinetics data confirm that protonation of the protease stabilizes the inhibitor/anion/enzyme ternary complex. A representative urea inhibitor (ACPU) shows a pH-dependent effect of sulfate on K_i (H^+/SO_4^{2-} effect). This H^+/SO_4^{2-} effect is not observed for control inhibitors such as benzamidine. In neutral conditions, neither ACPU nor benzamidine shows an effect of sulfate on K_i. Both inhibitors show a nominal 1−2-fold reduction of K_i upon addition of sulfate. However, in mildly acidic conditions, ACPU and benzamidine differ. ACPU, but not benzamidine, shows a substantial (5-fold) decrease in K_i upon addition of sulfate. The differences between ACPU and benzamidine indicate that constituents of ACPU beyond the amidinophenyl moiety are required for the H^+/SO_4^{2-} effect. The effect is not specific for sulfate. Our kinetics data indicate that other oxyanions such as phosphate can substitute for sulfate ion in the ternary inhibitor/oxyanion/protease complex.

This kinetics data, along with the three-dimensional structures of ternary inhibitor/sulfate/protease complexes and a previous observation that the pK_a of His 57 increases upon binding of noncovalent oxyanions [α-lytic protease (*42*)], support the following mechanism for the effect of H^+/SO_4^{2-} on K_i. Protonation of the Nϵ2 of His 57 unmasks the A_{Lig} position allowing an oxyanion such as sulfate or phosphate to bind to the trypsin active site. Oxyanions occupy the A_{Lig} and B_{Lig} positions, and are stabilized by hydrogen bonds to protons on His 57 Nϵ2, Ser 195 Oγ, and Gly 193 N and by electrostatic interactions with the His 57 cation. The protease S_1 pocket plus oxyanion combine to form a conjugated binding site, composed of direct and virtual functional groups. Inhibitors such as ACPU, with appropriate hydrogen bond donors, can bind to aspartate and sulfate in this conjugated binding site. Hence, the *protonated* ACPU−trypsin complex gains stability by recruiting a sulfate ion, which ligates enzyme and inhibitor together via electrostatics and a complex network of multiple-centered hydrogen bonds.

The Chemical Composition of Benzamidine-Based Inhibitors Modulates the H^+/SO_4^{2-} Effect. The effect of H^+/SO_4^{2-} on benzamidine-based derivatives described here is modulated by (i) the composition of the linker, (ii) the position of the linker on ring A with respect to the amidino group, and (iii) the hydrogen-bonding functionalities and electronic structure of the linker. To determine which structural constituents of an inhibitor contribute the H^+/SO_4^{2-} effect, we examined the effects of sulfate on K_is of a series of related inhibitors under acidic conditions (Table 4). The ether derivatives, which cannot form hydrogen bonds with proton acceptors, show no H^+/SO_4^{2-} effect. By contrast, selected urea derivatives, which are proton donors, show significant H^+/SO_4^{2-} effect. Comparison of the series of urea

inhibitors reveals that position of the urea group is important for the H^+/SO_4^{2-} effect. Substitution of the urea group para to the amidino group on ring A appears to appropriately position the hydrogen bond donors adjacent to sulfate oxyanions. For example, inhibitors **1** and **5** differ only by para (inhibitor **1**) versus meta (inhibitor **5**) substitution of ring A with the phenyl-urea group. Compound **1** shows a significant H^+/SO_4^{2-} effect while inhibitor **5** shows nominal effect. In addition, the H^+/SO_4^{2-} effect increases with the electron-withdrawing nature of substituents attached to the urea linker distal to the amidinophenyl moiety. For example, comparison of inhibitors **1** and **3** indicates that insertion of a methylene bridge between the phenyl substituent and urea linker lessens the H^+/SO_4^{2-} effect. A methylene group would insulate the urea group from the electron-withdrawing nature of the phenyl substituent. Electron-withdrawing groups on the urea linker should enhance the H^+/SO_4^{2-} effect by increasing the acidity of the urea amide protons, thereby strengthening hydrogen bonds with sulfate oxyanions. Comparing inhibitors **1** and ACPU indicates that adding a chlorine atom to the phenyl group on the urea linker increases the H^+/SO_4^{2-} effect. Adding an amidino group (inhibitor **11**) in this position increases the effect further. Chlorine would increase the electron-withdrawing nature of the phenyl group primarily through an inductive effect. The amidino group would accomplish the same via resonance. Conversely, adding a phenoxy group to the phenyl substituent at this same position lessens the effect (inhibitor **4**), consistent with the electron-releasing nature of the phenoxy group.

Cations and Anions Can Mediate Interaction of Inhibitors with Proteases. Cation mediation of potency of competitive inhibitors of serine proteases has been reported (*11*). The K_i values for a family of benzamidine-based inhibitors were determined for a variety of enzymes with assays performed in the presence or absence of divalent zinc ion. In addition, for one of the compounds [keto-BABIM, which is bis(5-amidino-2-benzimidazolyl)methane ketone], the three-dimensional structure of a ternary inhibitor/cation/trypsin complex grown under basic conditions shows an architecture similar to that described here. The zinc cation there appears to be in nearly the same location within the trypsin active site as the sulfate anion here. The zinc cation is tetrahedrally coordinated by Oγ of Ser 195 and *unprotonated* Nϵ2 of His 57, and two *unprotonated* imides in the keto-BABIM linker. In contrast, in acid conditions, sulfate oxyanions form hydrogen bonds to two *protonated* imides of BABIM, protons on His 57 Nϵ2, Ser 195 Oγ, and Gly 193 N, and two water molecules (*11*). These interactions are similar to those described here for ACPU, etc. The 6-fold improvement of BABIM potency for trypsin in acidic conditions and in the presence of sulfate is also consistent with our results.

Incorporating a sulfonyl or other oxyanionic functional group onto an inhibitor, to target conserved noncovalent oxyanion binding sites (the A_{Lig} and B_{Lig} positions), could increase their affinity for serine proteases. The utility of sulfate ion for improving potency of protease inhibitors in a physiological setting is doubtful, as the effect of sulfate ion is modest. By contrast, zinc ion at subphysiological concentrations (100 nM) reduces the K_i of BABIM for bovine trypsin from 19 μM to 5 nM (*11*). Our work, however, identifies trypsin-binding sites for noncovalent oxyanions (unmasked in acidic conditions), which may be conserved in other serine proteases. It is conceivable that an inhibitor covalently incorporating oxyanions for interaction with the A_{Lig} and B_{Lig} positions could bind tightly and induce protonation at physiological pH (*42*), shutting down catalysis.

Inhibitors Demonstrate Competitive, Micromolar Inhibition of Five Trypsin-like Enzymes. For substituted benzamidine inhibitors, bovine trypsin K_is have previously been shown to correlate with molecular weight and extent of hydrophobic interaction (*43*). We observe, for example, that trypsin K_i is decreased by (i) extending compound **1** by adding a phenoxy group to form APPU, (ii) replacing the chlorine substitutent of ACPU with a phenoxy group to form APPU, and (iii) adding a phenoxy group to compound **5** to form compound **6**. K_i values for the aryl inhibitors decrease with increasing hydrophobic interaction with trypsin surface residues.

No significant H^+/SO_4^{2-} effect is observed for compound **1** with thrombin, which shows a significant $H+/SO_4^{2-}$ effect with bovine trypsin (Table 4). For human thrombin, the urea derivatives with substituents para to the amidino group show weak potency (K_is $\approx$ 175$-$300 μM). The kinetics and modeling data both suggest that para-substituted compounds with urea linkers engage in unfavorable contacts with residues of the insertion loop in thrombin (Figure 4). Adding substituents of increasing size meta to the amidino group decreases the K_i for thrombin significantly, however. Adding a phenoxy group para to the urea linkage on ring B of compound **5** (ring B substituted meta to the amidino group on ring A) to form compound **6** decreases the K_i. Substituting a phenoxy group on ring B meta to the ether linkage of compound **9** to form compound **10** decreases the K_i even more significantly. Compound **10** is the most potent inhibitor for human thrombin in the series, with a potency approximately 75-fold greater than benzamidine ($K_i = 235$ μM, ref *5*). The extended aryl moieties of compound **10** may interact with some of the more hydrophobic binding sites (aryl, S2) of human thrombin (*33*).

In a molecular model of granzyme A (*44*), an aspartic acid residue at the bottom of the S_1 pocket is consistent with a preference for arginine and lysine at the substrate P_1 position (*45*). A notable difference in the active sites of trypsin and granzyme A is the change in residue 99 from Leu in trypsin to Lys in granzyme A. In trypsin, Leu 99 is located at the base of the shallow S_2 pocket. In the granzyme A model, Lys 99 essentially fills the S_2 pocket. These differences in residue 99 are consistent with the observed preference of Granzyme A for meta-substituted urea derivatives (inhibitors **5** and **6**) over para-substituted urea derivatives. The meta-substituted derivatives may have lower K_i values due to improved contacts with residues of the S_2 pocket. Unlike granzyme A, but like trypsin, meta- and para-substituted urea derivatives inhibit rat skin tryptase equally well (Table 2), suggesting that the S2 pocket of rat skin tryptase is more like that of bovine trypsin than of human granzyme A.

ACKNOWLEDGMENT

We thank Dr. Wolfram Bode for helpful discussions.

REFERENCES

1. Schecter, I., and Berger, A. (1967) *Biochem. Biophys. Res. Commun. 27*, 157−162.

2. Neurath, H. (1984) *Science 224*, 350−357.
3. Stroud, R. M. (1974) *Sci. Am. 231*, 74−88.
4. Powers, J. C., and Harper, J. W. (1986) in *Proteinase Inhibitors* (Barrett, A. J., Eds.) Vol. 12, pp 55−152, Elsevier, Amsterdam.
5. Geratz, J. D., Stevens, F. M., Polakoski, K. L., Parrish, R. F., and Tidwell, R. R. (1979) *Arch. Biochem. Biophys. 197*, 551−559.
6. Stürzbecher, J., Markwardt, F., Voigt, B., Wagner, G., and Walsmann, P. (1983) *Thromb. Res. 29*, 635−642.
7. Stürzebecher, J., Prasa, D., and Sommerhoff, C. (1992) *Hoppe-Seyler's Z. Physiol. Chem. 373*, 1025−1030.
8. Geratz, J. D., Cheng, M., and Tidwell, R. R. (1976) *J. Med. Chem. 19*, 634−639.
9. Krieger, M., Kay, L. M., and Stroud, R. M. (1974) *J. Mol. Biol. 83*, 209−230.
10. Bode, W., and Schwager, P. (1975) *J. Mol. Biol. 98*, 693−717.
11. Katz, B. A., Clark, J. M., Finer-Moore, J. S., Jenkins, T. E., Johnson, C. R., Ross, M. J., Luong, C., Moore, W. R., and Stroud, R. M. (1998) *Nature 391*, 608−612.
12. McRae, B. J., Kurachi, K., Heimark, R. L., Fujikawa, K., Davie, E. W., and Powers, J. C. (1981) *Biochemistry 20*, 7196−7206.
13. Ashley, J. N., Barber, H. J., Ewins, A. J., Newbery, G., and Self, A. D. H. (1942) *J. Chem. Soc.* 103−116.
14. Dixon, M. (1953) *Biochem. J. 55*, 170.
15. Kam, C.-M., Hernandez, M. A., Patil, G. S., Ueda, T., Simmons, W. H., Braganza, V. J., and Powers, J. C. (1995) *Arch. Biochem. Biophys. 316*, 808−814.
16. Schroeder, D. D., and Shaw, E. (1968) *J. Biol. Chem. 243*, 2943−2949.
17. Xuong, N. H., Nielsen, C., Hamlin, R., and Anderson, D. (1985) *J. Appl. Crystallogr. 18*, 342−350.
18. Brunger, A., Kuriyan, J., and Karplus, M. (1987) *Science 235*, 458−460.
19. Bode, W., and Schwager, P. (1975) *FEBS Lett. 56*, 139−143.
20. Brooks, B. R., Bruccoleri, R. E., Olafson, B. D., States, D. J., Swaminathan, S., and Karplus, M. (1983) *J. Comput. Chem 4*, 187−217.
21. Piskov, V. B., Kasperovich, V. P., Tsvetkov, E. I., Khvalkovskaya, A. V., Koblova, I. A., and Poluektov, V. S. (1974) *Khim.-Farm. Zh. 8*, 17−20.
22. Sweet, R. M., Wright, H. T., Janin, J., Chothia, C. H., and Blow, D. M. (1974) *Biochemistry 13*, 4212−4228.
23. Walter, J., and Bode, W. (1983) *Hoppe-Seyler's Z. Physiol. Chem. 364*, 949−959.
24. Lee, A. Y., Hagihara, M., Karmacharya, R., Albers, M. W., Schreiber, S. L., and Clardy, J. (1993) *J. Am. Chem. Soc. 115*, 12619−12620.
25. Bode, W., Turk, D., and Stürzebecher, J. (1990) *Eur. J. Biochem. 193*, 175−182.
26. Bode, W., Ulrich, I., Baumann, U., Huber, R., Stone, S. R., and Hofsteenge, J. (1989) *EMBO J. 8*, 3467−3475.
27. Taylor, R., Kennard, O., and Versichel, W. (1984) *J. Am. Chem. Soc. 106*, 244−248.
28. Jeffrey, G. A., and Mitra, J. (1984) *J. Am. Chem. Soc. 106*, 5546−5553.
29. Bernstein, F. C., Koetzle, T. F., Williams, J. G. B., Meyer, E. F., Brice, M. D., Rodgers, J. R., Kennard, O., Shimanouchi, T., and Tasumi, M. (1977) *J. Mol. Biol. 112*, 535−542.
30. Bartunik, H. D., Summers, L. J., and Bartsch, H. H. (1989) *J. Mol. Biol. 210*, 813−828.
31. Jeffrey, G. A. (1997) *An Introduction to Hydrogen Bonding*, Oxford University Press, New York.
32. Fujinaga, M., Delbaere, L. T., Brayer, G. D., and James, M. N. (1985) *J. Mol. Biol. 184*, 479−502.
33. Bode, W., Turk, D., and Karshikov, A. (1992) *Protein Sci. 1*, 426−471.
34. Perona, J. J., and Craik, C. S. (1995) *Protein Sci. 4*, 337−360.
35. Earnest, T., Fauman, E., Craik, C. S., and Stroud, R. (1991) *Proteins 10*, 171−187.
36. Tsukada, H., and Blow, D. M. (1985) *J. Mol. Biol. 184*, 703−711.
37. Blevins, R. A., and Tulinsky, A. (1985) *J. Biol. Chem. 260*, 4264−4275.
38. Goddette, D. W., Paech, C., Yang, S. S., Mielenz, J. R., Bystroff, C., Wilke, M. E., and Fletterick, R. J. (1992) *J. Mol. Biol. 228*, 580−595.
39. Berglund, G. I., Smalas, A. O., Outzen, H., and Willassen, N. P. (1998) *Mol. Mar. Biol. Biotechnol. 7*, 105−114.
40. Kraut, J. (1977) *Annu. Rev. Biochem. 46*, 331−358.
41. Polgar, L. (1989) *Mechanisms of Protease Action*, Chapter 3, CRC Press, Boca Raton.
42. Smith, S. O., Farr-Jones, S., Griffin, R. G., and Bachovchin, W. W. (1989) *Science 244*, 961−964.
43. Andrews, J. M., Roman, D. P., and Bing, D. H. (1978) *J. Med. Chem. 21*, 1202−1207.
44. Murphy, M. E. P., Moult, J., Bleackley, R. C., Gershenfeld, H., Weissman, I. L., and James, M. N. G. (1988) *Proteins 4*, 190−204.
45. Odake, S., Kam, C. M., Narasimhan, L., Poe, M., Blake, J. T., Krahenbuhl, O., Tschopp, J., and Powers, J. C. (1991) *Biochemistry 30*, 2217−2227.
46. Smalas, A. O., Heimstad, E. S., Hordvik, A., Willassen, N. P., and Male, R. (1994) *Proteins 20*, 149−166.
47. Mattos, C., Rasmussen, B., Ding, X., Petsko, G. A., and Ringe, D. (1994) *Nat. Struct. Biol. 1*, 55−58.
48. Ding, X., Rasmussen, B. F., G. A., P., and Ringe, D. (1994) *Biochemistry 33*, 9285−9293.
49. Meyer, E., Cole, G., Radhakrishnan, R., and Epp, O. (1988) *Acta Crystallogr., Sect. B 44*, 26−38.
50. Mace, J. E., and Agard, D. A. (1995) *J. Mol. Biol. 254*, 720−736.
51. Rader, S. D., and Agard, D. A. (1997) *Protein Sci. 6*, 1375−1386.
52. Katz, B. A., Finer-Moore, J., Mortezaei, R., Rich, D. H., and Stroud, R. M. (1995) *Biochemistry 34*, 8264−8289.
53. Weber, P. C., Lee, S. L., Lewandowski, F. A., Schadt, M. C., Chang, C. W., and Kettner, C. A. (1995) *Biochemistry 34*, 3750−3757.
54. Bone, R., Frank, D., Kettner, C. A., and Agard, D. A. (1989) *Biochemistry 28*, 7600−7609.
55. Stoll, V. S., Eger, B. T., Hynes, R. C., Martichonok, V., Jones, J. B., and Pai, E. F. (1998) *Biochemistry 37*, 451−462.
56. Bertrand, J. A., Oleksyszyn, J., Kam, C. M., Boduszek, B., Presnell, S., Plaskon, R., Suddath, F. L., Powers, J. C., and Williams, L. D. (1996) *Biochemistry 35*, 3147−3155.

BI981636U